Mycophenolic anilides as broad specificity inosine-5'-monophosphate dehydrogenase (IMPDH) inhibitors

Seungheon Lee[a], **Angela Ku**[a,b], **Mohana Rao Vippila**[a], **Yong Wang**[a], **Minjia Zhang**[c], **Xingyou Wang**[c], **Lizbeth Hedstrom**[c,d], **Gregory D. Cuny**[a,*]

[a]Department of Pharmacological and Pharmaceutical Sciences, University of Houston, Health Building 2, Houston, Texas 77204, USA

[b]Department of Chemistry, University of Houston, Health Building 2, Houston, Texas 77204, USA

[c]Department of Biology, 415 South St., Waltham, MA 02454, USA

[d]Department of Chemistry, Brandeis University, 415 South St., Waltham, MA 02454, USA

Abstract

Inosine-5'-monophosphate dehydrogenase (IMPDH) is a potential target for microorganisms. However, identifying inhibitor design determinants for IMPDH orthologs continues to evolve. Herein, a series of mycophenolic anilide inhibitors of *Cryptosporidium parvum* and human IMPDHs are reported. Furthermore, molecular docking of **12** (e.g. SH-19; *Cp*IMPDH $K_{i,app}$ = 0.042 ± 0.015 μM, *Hs*IMPDH2 $K_{i,app}$ = 0.13 ± 0.05 μM) supports different binding modes with the two enzymes. For *Cp*IMPDH the inhibitor extends into a pocket in an adjacent subunit. In contrast, the inhibitor interacts with Ser276 in the NAD binding site in *Hs*IMPDH2, as well as an adjacent pocket within the same subunit. These results provide further guidance for generating IMPDH inhibitors for enzymes found in an array of pathogenic microorganisms, including *Mycobacterium tuberculosis*.

Graphical Abstract

[*]Corresponding author at: Department of Pharmacological and Pharmaceutical Sciences, University of Houston, Health Building 2, Houston, Texas 77204, USA (G.D. Cuny). gdcuny@central.uh.edu (G.D. Cuny).
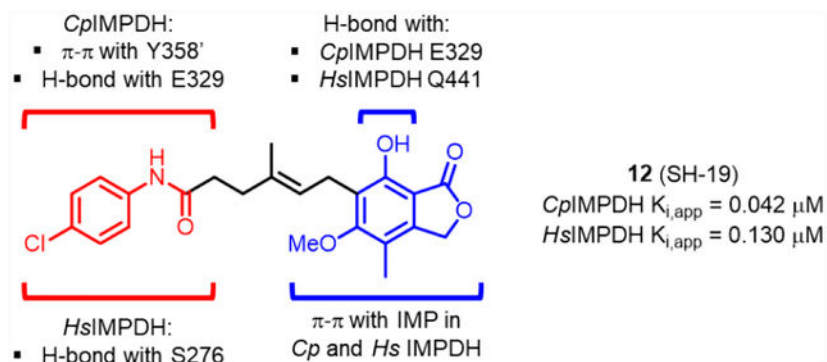
Appendix A. Supplementary data

Supplementary data to this article can be found online at.

CpIMPDH:
- π-π with Y358'
- H-bond with E329

H-bond with:
- CpIMPDH E329
- HsIMPDH Q441

HsIMPDH:
- H-bond with S276

π-π with IMP in Cp and Hs IMPDH

12 (SH-19)
$CpIMPDH\ K_{i,app} = 0.042\ \mu M$
$HsIMPDH\ K_{i,app} = 0.130\ \mu M$

Keywords

Cryptosporidium parvum ; IMPDH; Inosine-5'-monophosphate dehydrogenase; Inhibitor; Binding mode

Inosine-5'-monophosphate dehydrogenase (IMPDH) catalyzes the nicotinamide adenine dinucleotide (NAD)-dependent oxidation of inosine 5'-monophosphate (IMP) to xanthosine 5'-monophosphate (XMP) as the rate-limiting step in the biosynthesis of guanine nucleotides.[1] Therefore, IMPDH regulates intracellular guanine nucleotide pools and is critical for cell proliferation in both eukaryotes and prokaryotes.[2]

IMPDH inhibition has recently gained momentum as a potential treatment of microbial infections. For example, blocking prokaryotic IMPDH could provide a strategy for growth inhibition of bacteria such as *Mycobacterium tuberculosis* (*Mtb*) and *Staphylococcus aureus* (*Sa*).[3, 4] In addition, this enzyme has been targeted in the protozoan *Cryptosporidium parvum* (*Cp*), which has a similar IMPDH to some prokaryotes, likely resulting from lateral gene transfer from bacteria.[5, 6] These prokaryotic IMPDHs are structurally distinct from their human counterparts.[2] The most dramatic difference is in the adenosine subsite (A-site) of the NAD binding site[7, 8], and several inhibitor scaffolds (e.g. **1** – **6** in Figure 1A) exploit this divergence.[9–17]

Mycophenolic acid (MPA, **7**, Figure 1B) is a prototypic human (*Hs*) IMPDH inhibitor[18, 19] (e.g. $HsIMPDH1\ K_i = 33$ nM and $HsIMPDH2\ K_i = 7$ nM)[20] used clinically as an ester prodrug (e.g. mycophenolate mofetil) for immunosuppression in preventing rejection following organ transplantation.[21] Interestingly, MPA (**7**) binds in the nicotinamide subsite, but is a poor inhibitor of prokaryotic and *C. parvum* IMPDHs (e.g. $CpIMPDH\ K_i = 9.3$ μM).[22] Mycophenolic anilides have also been found to inhibit *Hs*IMPDH2,[23–25] but their activities against *Cp*IMPDH and bacterial orthologs have not been described.

Herein, we report a structure-activity relationship study for a series of mycophenolic anilides that incorporate a molecular fragment common to several classes of *Cp*IMPDH inhibitors (Figure 1C). Furthermore, an analysis of these anilides was conducted to elucidate additional structural determinants required for selective inhibition of *Cp*IMPDH and related prokaryotic orthologs versus *Hs*IMPDHs.

An initial set of MPA-anilide derivatives **8** – **16** were prepared via EDC-mediated coupling (Scheme 1). In addition, **10** was further modified by phenol alkylation or alkene reduction to provide derivatives **17** and **18**, respectively.[28]

Replacement of the alkene with a cyclopropane bioisostere was also pursued. The synthesis of both enantiomers is illustrated in Schemes 2 and 3. MPA (**7**) was converted to aldehyde **19**,[23] which was protected and then reduced to provide alcohol **21** (Scheme 2). A chiral auxiliary was attached generating key intermediate **23a** using the methodology of Charette et al.[29, 30] Finally, anomerization generated a second crucial intermediate **23b**. Both of these intermediates were partially de-protected generating **24a** and **24b**, which were subjected to cyclopropanation conditions to give **25a** and **25b**, respectively (Scheme 3).[31, 32] These two materials were then subjected to a similar series of transformations (Scheme 4).[33, 34] The chiral auxiliary was removed followed by alcohol oxidation, Horner-Wadsworth-Emmons reactions and alkene reduction to produce **29a** and **29b**. Finally, ester hydrolysis and EDC-mediated aniline coupling provided **31a** and **31b**.

Several other derivatives were prepared that incorporated additional changes to the linker region of the hybrid molecules. MPA (**7**) was cleaved to aldehyde **32**, which was reduced and protected to give **34** (Scheme 5). Alkylation of the primary alcohol, ester hydrolysis, aniline coupling and deprotection produced the ether linked derivative **38**.[35] MPA (**7**) was also converted to aldehyde **40a**, which via a Wittig reaction with 4-ClPhNH(C=O)CH$_2$P$^+$Ph$_3$Cl$^-$ gave **41a** (Scheme 6).[36, 37] Similarly, **34** was oxidized to aldehyde **40b**, which was converted into **41b**. These two intermediates were de-protected or reduced/de-protected to provide **42a** and **42b**, respectively. Finally, intermediate **32** was oxidized to carboxylic acid **43**, which was coupled to 4-chloroaniline to give the truncated derivative **44** (Scheme 7).

Recombinant *Cp*IMPDH and *Hs*IMPDH2 were purified from *E. coli*.[38] Enzyme activity was determined by monitoring the production of NADH.[39] For *Cp*IMPDH, enzyme (10 nM) and inhibitor (1 nM to 5 μM) were incubated in the presence of 50 mM Tris-HCl, pH 8.0, 100 mM KCl, 3 mM EDTA, 1 mM dithiothreitol at 25 °C for 5 min prior to addition of substrates NAD (300 μM) and IMP (250 μM). For *Hs*IMPDH2, enzyme (20 nM) and inhibitor (1 nM to 5 μM) were incubated in the presence of 50 mM Tris-HCl, pH 8.0, 100 mM KCl, 3 mM EDTA, 1 mM dithiothreitol at 25 °C for 5 min prior to addition of substrates NAD (60 μM) and IMP (250 μM).[41] Production of NADH was monitored by fluorescence. $K_{i,app}$ values were determined for each inhibitor against *Cp*IMPDH and *Hs*IMPDH2 using Dynafit.[40]

Introducing an anilide as the common fragment to MPA improved *Cp*IMPDH inhibition. For example, **8**, which incorporated the anilide from **4** with MPA, potently inhibited *Cp*IMPDH with $K_{i,app}$ value of 0.046 μM (Table 1). Interestingly, the compound also inhibited *Hs*IMPDH2 ($K_{i,app}$ = 0.35 μM), in contrast to all prior reported *Cp*IMPDH inhibitors. Since electron withdrawing groups were preferred in previously developed *Cp*IMPDH inhibitors, the methoxy group in **8** was replaced with a chloro (**9**). This compound showed similar inhibitory potency as **8** for both enzymes. However, replacing with a trifluoromethyl (**10**) increased potency against both enzymes. Transposing the *para*-chloro to the *ortho*-position

(**11**) resulted in loss of *Cp*IMPDH inhibitory activity. This was consistent with the SAR of other *Cp*IMPDH inhibitors, possibly resulting from a clash with Y358' and loss of a halogen bond with G357'.[9] A survey of various electron withdrawing groups at the 4-position demonstrated that chloro (**12**) provided potent and balanced *Cp*IMPDH and *Hs*IMPDH2 inhibition. Reminiscent of other *Cp*IMPDH inhibitors, methylation of the anilide (**16**) resulted in loss of activity. Similarly, methylation of the phenol (**17**), known to eliminate MPA inhibition of *Hs*IMPDH,[41] also resulted in loss of *Cp*IMPDH inhibition.

Next, the central linker was explored using various bioisosteres and by truncation (Table 2). 3-Trifluoromethyl-4-chloro or 4-chloro substituted anilides were chosen based on **10** and **12**. Reduction of the alkene (**18**) resulted in some loss of potency for *Cp*IMPDH inhibition, which was more dramatic for *Hs*IMPDH2. Bioisosteric replacement of the alkene with a cyclopropane revealed that one enantiomer (**31b**) retained potent *Cp*IMPDH inhibitory activity ($K_{i,app} = 0.066$ μM), although *Hs*IMPDH2 inhibition was reduced ($K_{i,app} = 0.46$ μM). The eudysmic ratios of **31b** and **31a** for *Cp*IMPDH and *Hs*IMPDH inhibitions were 8.6 and 3.1, respectively. Several additional changes to the linker connecting the two aryl groups resulted in reduced *Cp*IMPDH and *Hs*IMPDH2 inhibitory activities.

Two critical differences between *Hs*IMPDH2 and *Cp*IMPDH are in a loop structure of the NAD binding region and a proximal site in the adjacent subunit. The A-site of *Hs*IMPDH2 is largely within the same monomer as the IMP site, but for *Cp*IMPDH and related prokaryotic IMPDHs, a portion of the A-site is located in the adjacent subunit.[7, 8] This hydrophobic pocket is absent in *Hs*IMPDH.[42] As illustrated in the sequence alignments of *Hs*IMPDH2 and *Cp*IMPDH (Figure 2), the NAD loop of *Hs*IMPDH contains a hydrophilic serine at residue 276, while *Cp*IMPDH has a hydrophobic alanine at the equivalent position (residue 165'; note that *Cp*IMPDH lacks an approximately 100 residue regulatory domain present in most IMPDHs). For the A-site, there are also distinct residue differences with aspartic acid (e.g. 470') in *Hs*IMPDH corresponding to tyrosine (e.g. Y358') in *Cp*IMPDH.[42] Interaction with this tyrosine residue has previously been shown to be critical for achieving selective *Cp*IMPDH inhibitors.[9–17, 27] Interestingly, a number of other microorganisms, including several pathogenic Gram-(+) and Gram-(−) bacteria listed in Figure 2, also have alanine and tyrosine residues in these two positions and are inhibited by *Cp*IMPDH inhibitors.[27]

In order to understand potential binding modes of MPA-anilides to *Cp*IMPDH and *Hs*IMPDH, molecular docking studies were conducted using Autodock Tools. Docking of **12** into *Cp*IMPDH (PDB: 3KHJ) provided a low energy pose that satisfied the three key interactions of previously co-crystalized selective *Cp*IMPDH inhibitors. Specifically, the phenol portion of MPA had a π-π interaction with the hypoxanthine of IMP, the anilide NH formed a hydrogen bond with Glu329 and the anilide extended into the adjacent subunit forming a π-π interaction with Tyr358' (Figure 3A). Additionally, the phenol OH formed an ionic-dipole interaction with Glu329. This binding mode is also consistent with several of the observed structure-activity relationship features, such as alkylation of the anilide or phenol disrupting interactions with Glu329. In addition, truncation of the linker would result in an inability of the inhibitor to extend into the other subunit to provide the critical π-π interaction with Tyr358'. Overlay of this docking model with the co-crystal structure of *Cp*IMPDH•IMP•**5** (PDB: 4RVB) further illustrates that **12** can readily be accommodated

in a binding mode similar to selective *Cp*IMPDH inhibitors (see Supporting Information, Figure S1A).[10]

Docking of **12** into hamster IMPDH2 (PDB : 1JR1), which has only eight non-binding site amino acid differences[43] compared to *Hs*IMPDH2, provided a low energy pose with similar interactions as MPA (**7**), including H-bonding of the anilide NH and phenol to Ser276 in the NAD binding site and Gln441, respectively (Figure 3B; for an overlay of the docked structure of **12** with hamster IMPDH2•IMP•**7** see Supporting Information, Figure S1B). The *para*chlorophenyl occupies a modestly large pocket created by Thr252, His253, Phe282 and Ser275, as well as being within 3.2 Å of the methylene portion of this later residue's side-chain. Interestingly, attempts to dock a *Cp*IMPDH selective inhibitor (e.g. **5**) into hamster IMPDH2 did not produce reasonable binding modes with low binding energies (data not shown). This could result from the compound being less flexible and not being able to form a productive interaction with Ser276 in the NAD site. Collectively, these data elucidated an additional structural criterion for achieving *Cp*IMPDH inhibitor selectivity: the inability to form interactions with Ser276.

Since MPA anilides inhibit *Cp*IMPDH, we also assessed inhibition of *Mycobacterium tuberculosis* (*Mtb*) IMPDH that likewise has alanine in the NAD loop and tyrosine in the A-site (Figure 2). Similar to other active *Cp*IMPDH inhibitors, compound **10** potently blocked *Mtb*IMPDH ($K_{i,app}$ = 0.060 μM).

In conclusion, mycophenolic anilides were found that inhibit both *Cp*IMPDH and *Hs*IMPDH by incorporation of a molecular fragment from previously reported *Cp*IMPDH inhibitors. Prior studies combined with molecular docking assessments revealed that selectivity for microorganism IMPDHs (e.g. those with alanine in the NAD loop and Y358' in the adjacent subunit) requires two distinct design elements: 1) interaction with the adjacent subunit via π-π interactions with Y358' and 2) lack of interactions with Ser276 in the NAD binding site of *Hs*IMPDH. These two features provide further guidance for generating selective IMPDH inhibitors for a subset of susceptible microorganisms.

Supplementary Material

Refer to Web version on PubMed Central for supplementary material.

Acknowledgements

References

1. Hedstrom L IMP dehydrogenase: structure, mechanism, and inhibition. Chem Rev. 2009;109(7): 2903–2928. [PubMed: 19480389]

2. Hedstrom L, Liechti G, Goldberg JB, Gollapalli DR. The antibiotic potential of prokaryotic IMP dehydrogenase inhibitors. Curr Med Chem. 2011;18(13): 1909–1918. [PubMed: 21517780]

3. Makowska-Grzyska M, Kim Y, Gorla SK, et al. Mycobacterium tuberculosis IMPDH in Complexes with Substrates, Products and Antitubercular Compounds. PLoS One. 2015;10(10): e0138976. [PubMed: 26440283]

4. Yeswanth S, Kumar CL, Swarupa V, et al. Characterization of inosine monophosphate dehydrogenase from Staphylococcus aureus ATCC12600 and its involvement in biofilm formation. 2013;11: 12.

5. Striepen B, Pruijssers AJ, Huang J, et al. Gene transfer in the evolution of parasite nucleotide biosynthesis. Proc Natl Acad Sci U S A. 2004;101(9): 3154–3159. [PubMed: 14973196]

6. Striepen B, White MW, Li C, et al. Genetic complementation in apicomplexan parasites. Proc Natl Acad Sci U S A. 2002;99(9): 6304–6309. [PubMed: 11959921]

7. Makowska-Grzyska M, Kim Y, Maltseva N, et al. A novel cofactor-binding mode in bacterial IMP dehydrogenases explains inhibitor selectivity. J Biol Chem. 2015;290(9): 5893–5911. [PubMed: 25572472]

8. Colby TD, Vanderveen K, Strickler MD, Markham GD, Goldstein BM. Crystal structure of human type II inosine monophosphate dehydrogenase: implications for ligand binding and drug design. Proc Natl Acad Sci U S A. 1999;96(7): 3531–3536. [PubMed: 10097070]

9. Sun Z, Khan J, Makowska-Grzyska M, et al. Synthesis, in vitro evaluation and cocrystal structure of 4-oxo-[1]benzopyrano[4,3-c]pyrazole Cryptosporidium parvum inosine 5'-monophosphate dehydrogenase (CpIMPDH) inhibitors. J Med Chem. 2014;57(24): 10544–10550. [PubMed: 25474504]

10. Kim Y, Makowska-Grzyska M, Gorla SK, et al. Structure of Cryptosporidium IMP dehydrogenase bound to an inhibitor with in vivo antiparasitic activity. Acta Crystallogr F Struct Biol Commun. 2015;71(Pt 5): 531–538. [PubMed: 25945705]

11. Johnson CR, Gorla SK, Kavitha M, et al. Phthalazinone inhibitors of inosine-5'-monophosphate dehydrogenase from Cryptosporidium parvum. Bioorg Med Chem Lett. 2013;23(4): 1004–1007. [PubMed: 23324406]

12. Gorla SK, Kavitha M, Zhang M, et al. Optimization of benzoxazole-based inhibitors of Cryptosporidium parvum inosine 5'-monophosphate dehydrogenase. J Med Chem. 2013;56(10): 4028–4043. [PubMed: 23668331]

13. Kirubakaran S, Gorla SK, Sharling L, et al. Structure-activity relationship study of selective benzimidazole-based inhibitors of Cryptosporidium parvum IMPDH. Bioorg Med Chem Lett. 2012;22(5): 1985–1988. [PubMed: 22310229]

14. Gorla SK, Kavitha M, Zhang M, et al. Selective and potent urea inhibitors of cryptosporidium parvum inosine 5'-monophosphate dehydrogenase. J Med Chem. 2012;55(17): 7759–7771. [PubMed: 22950983]

15. Sharling L, Liu X, Gollapalli DR, Maurya SK, Hedstrom L, Striepen B. A screening pipeline for antiparasitic agents targeting cryptosporidium inosine monophosphate dehydrogenase. PLoS Negl Trop Dis. 2010;4(8): e794. [PubMed: 20706578]

16. Gollapalli DR, Macpherson IS, Liechti G, Gorla SK, Goldberg JB, Hedstrom L. Structural determinants of inhibitor selectivity in prokaryotic IMP dehydrogenases. Chem Biol. 2010;17(10): 1084–1091. [PubMed: 21035731]

17. Maurya SK, Gollapalli DR, Kirubakaran S, et al. Triazole inhibitors of Cryptosporidium parvum inosine 5'-monophosphate dehydrogenase. J Med Chem. 2009;52(15): 4623–4630. [PubMed: 19624136]

18. Hager PW, Collart FR, Huberman E, Mitchell BS. Recombinant human inosine monophosphate dehydrogenase type I and type II proteins. Purification and characterization of inhibitor binding. Biochem Pharmacol. 1995;49(9): 1323–1329. [PubMed: 7763314]

19. Franklin TJ, Cook JM. The inhibition of nucleic acid synthesis by mycophenolic acid. Biochem J. 1969;113(3): 515–524. [PubMed: 5807210]

20. Carr SF, Papp E, Wu JC, Natsumeda Y. Characterization of human type I and type II IMP dehydrogenases. J Biol Chem. 1993;268(36): 27286–27290. [PubMed: 7903306]

21. van Gelder T, Hesselink DA. Mycophenolate revisited. Transpl Int. 2015;28(5): 508–515. [PubMed: 25758949]

22. Umejiego NN, Li C, Riera T, Hedstrom L, Striepen B. Cryptosporidium parvum IMP dehydrogenase: identification of functional, structural, and dynamic properties that can be exploited for drug design. J Biol Chem. 2004;279(39): 40320–40327. [PubMed: 15269207]

23. Pankiewicz KW, Lesiak-Watanabe KB, Watanabe KA, et al. Novel mycophenolic adenine bis(phosphonate) analogues as potential differentiation agents against human leukemia. J Med Chem. 2002;45(3): 703–712. [PubMed: 11806722]

24. Chen L, Wilson D, Jayaram HN, Pankiewicz KW. Dual inhibitors of inosine monophosphate dehydrogenase and histone deacetylases for cancer treatment. J Med Chem. 2007;50(26): 6685–6691. [PubMed: 18038969]

25. Shah CP, Kharkar PS. Newer human inosine 5'-monophosphate dehydrogenase 2 (hIMPDH2) inhibitors as potential anticancer agents. J Enzyme Inhib Med Chem. 2018;33(1): 972–977. [PubMed: 29792360]

26. Cuny GD, Suebsuwong C, Ray SS. Inosine-5'-monophosphate dehydrogenase (IMPDH) inhibitors: a patent and scientific literature review (2002–2016). Expert Opin Ther Pat. 2017;27(6): 677–690. [PubMed: 28074661]

27. Mandapati K, Gorla SK, House AL, et al. Repurposing cryptosporidium inosine 5'-monophosphate dehydrogenase inhibitors as potential antibacterial agents. ACS Med Chem Lett. 2014;5(8): 846–850. [PubMed: 25147601]

28. Li J, Wang S, Crispino GA, Tenhuisen K, Singh A, Grosso JAJTl. Selective removal of a benzyl protecting group in the presence of an aryl chloride under gaseous and transfer hydrogenolysis conditions. Tetrahedron Lett. 2003;44(21): 4041–4043.

29. Charette AB, Turcotte N, Côté BJJocc. One-pot synthesis of substituted allyl-α-D-glucopyranosides by an in situ anomerization protocol. J Carbohydr Chem. 1994;13(3): 421–432.

30. Pilgrim W, Murphy PV. SnCl(4)- and TiCl(4)-catalyzed anomerization of acylated O- and S-glycosides: analysis of factors that lead to higher alpha:beta anomer ratios and reaction rates. J Org Chem. 2010;75(20): 6747–6755. [PubMed: 20836488]

31. Charette AB, Turcotte N, Marcoux J-FJTl. The use of α-d-glucopyranosides as surrogates for the β-l-glucopyranosides in the stereoselective cyclopropanation reaction. Tetrahedron Lett. 1994;35(4): 513–516.

32. Charette AB, Cote BJJotACS. Stereoselective synthesis of all four isomers of coronamic acid: a general approach to 3-methanoamino acids. J Am Chem Soc. 1995;117(51): 12721–12732.

33. Charette AB, Cote BJTJoOC. Asymmetric cyclopropanation of allylic ethers: cleavage and regeneration of the chiral auxiliary. J Org Chem. 1993;58(4): 933–936.

34. Vega-Pérez JM, Periñán I, Palo-Nieto C, Vega-Holm M, Iglesias-Guerra FJTA. Alkenyl β-dgalactopyranoside derivatives as efficient chiral templates in stereoselective cyclopropanation and epoxidation reactions. Tetrahedron-Asymmetry. 2010;21(1): 81–95.

35. Krishna PR, Prapurna YL, Alivelu MJTl. InCl3 catalyzed carbene insertion into O–H bonds: efficient synthesis of ethers. Tetrahedron Lett. 2011;52(27): 3460–3462.

36. Zhaowen L, Li Z, Chunfen X, Yong Y, Fanbo Z, Kaixun HJMCR. Anticancer activities of some arylcarbamoylalkyltriphenylphosphonium chlorides. Med Chem Res. 2007;16(7–9): 380–391.

37. Soli ED, Braun MPJJoLC, Society RTOJotII. Synthesis of [phenyl-U-14C] aryl and [8–14C] carboxy labeled tracers of vorinostat. J Labelled Compd Rad. 2006;49(5): 437–443.

38. Umejiego NN, Gollapalli D, Sharling L, et al. Targeting a prokaryotic protein in a eukaryotic pathogen: identification of lead compounds against cryptosporidiosis. Chem Biol. 2008;15(1): 70–77. [PubMed: 18215774]

39. Farazi T, Leichman J, Harris T, Cahoon M, Hedstrom L. Isolation and characterization of mycophenolic acid-resistant mutants of inosine-5'-monophosphate dehydrogenase. J Biol Chem. 1997;272(2): 961–965. [PubMed: 8995388]

40. Kuzmic P Program DYNAFIT for the analysis of enzyme kinetic data: application to HIV proteinase. Anal Biochem. 1996;237(2): 260–273. [PubMed: 8660575]

41. Mitsuhashi S, Takenaka J, Iwamori K, Nakajima N, Ubukata M. Structure-activity relationships for inhibition of inosine monophosphate dehydrogenase and differentiation induction of K562 cells among the mycophenolic acid derivatives. Bioorg Med Chem. 2010;18(22): 8106–8111. [PubMed: 20934342]

42. Macpherson IS, Kirubakaran S, Gorla SK, et al. The structural basis of Cryptosporidium -specific IMP dehydrogenase inhibitor selectivity. J Am Chem Soc. 2010;132(4): 1230–1231. [PubMed: 20052976]

43. Collart FR, Huberman E. Cloning and sequence analysis of the human and Chinese hamster inosine-5'-monophosphate dehydrogenase cDNAs. J Biol Chem. 1988;263(30): 15769–15772. [PubMed: 2902093]
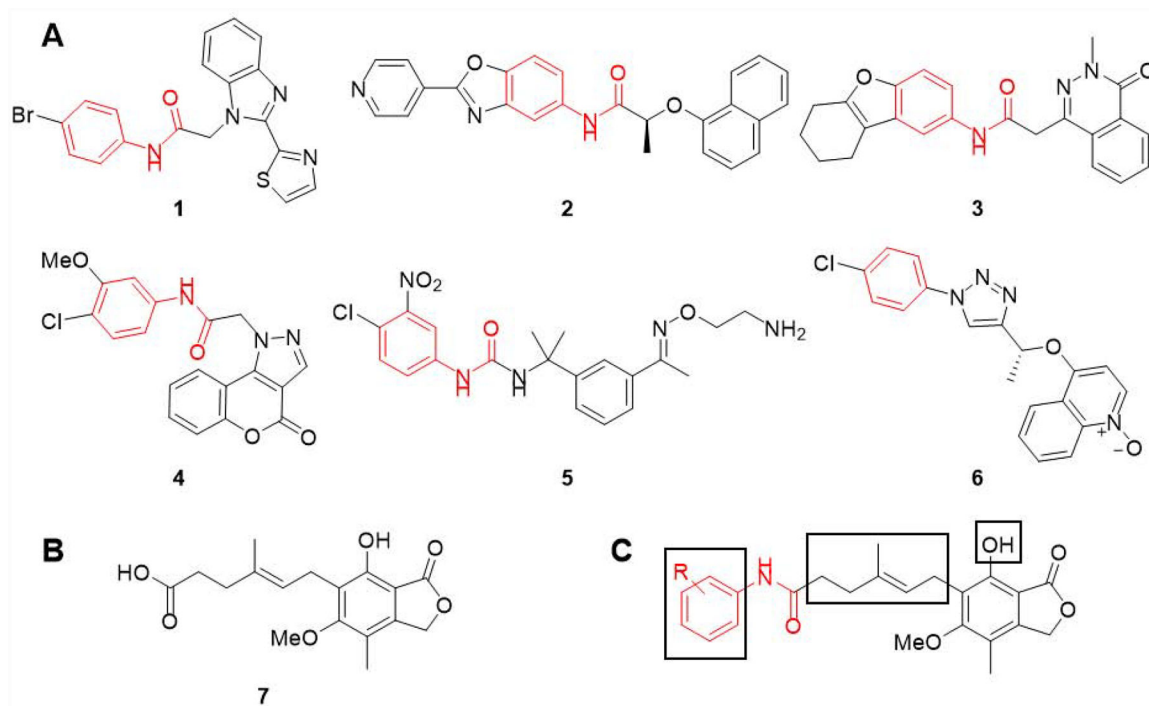
Figure. 1.

(**A**) Six structurally distinct *Cp*IMPDH inhibitors (*Cp*IMPDH IC$_{50}$ = 12 – 64 nM).[27] The fragments found in these inhibitors that interact with the adenosine subsite (A-site) of the NAD binding site are highlighted in red. This is based on co-crystal structures of **1**, **2**, **4** and **5** with *Cp*IMPDH and **6** with *Clostridium perfringens* IMPDH (*Clp*IMPDH). The interactions of inhibitor **3** are assumed based on structural similarity since it has not been co-crystalized with an IMPDH. (**B**) Structure of mycophenolic acid (MPA, **7**). (**C**) Mycophenolic anilides with three regions explored herein shown in boxes.

Figure. 2.

Sequence alignment of IMPDH enzymes from human, *C. parvum* and several bacteria highlighting the NAD loop and A-site. [a]Y358' is based on numbering for *Cp*IMPDH and the ' denotes the adjacent subunit.
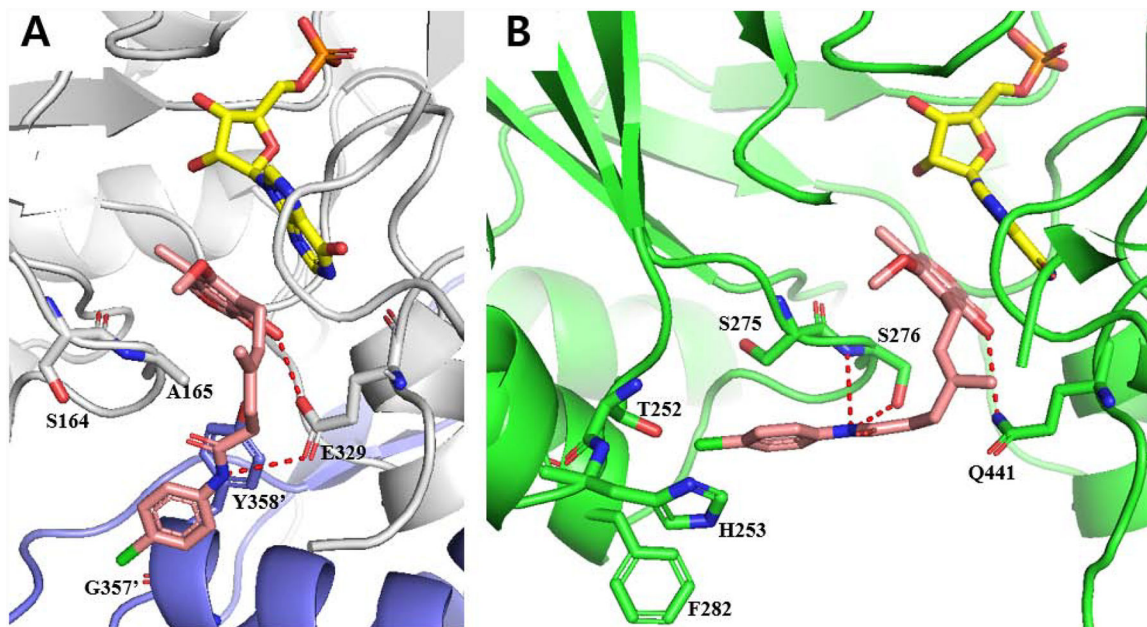
Figure 3.
(**A**) Docked model of **12** (pink) with *Cp*IMPDH (gray, PDB: 3KHJ) and IMP (yellow). Adjacent monomer protein is shown as purple and residue numbers are differentiate by prime ('). Hydrogen bonds are shown as red dashes (< 3.0 Å). Docking score of **12** with *Cp*IMPDH•IMP was −9.86. (**B**) Docked structure of **12** (pink) with hamster IMPDH2 (green, PDB: 1JR1) and IMP (yellow), which has only eight non-binding site amino acid differences compared to *Hs*IMPDH2[43]. Hydrogen bonds are shown as red dashes (< 3.5 Å). Docking score of **12** with hamster IMPDH2•IMP was −8.83. Water, K$^+$ and other protein subunits were deleted for docking and presentation for clarity.
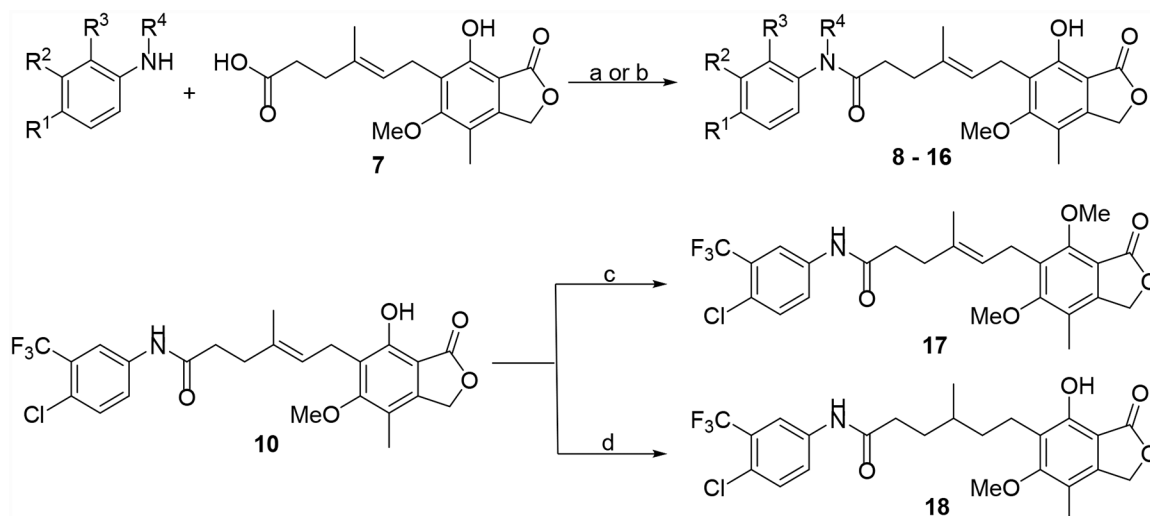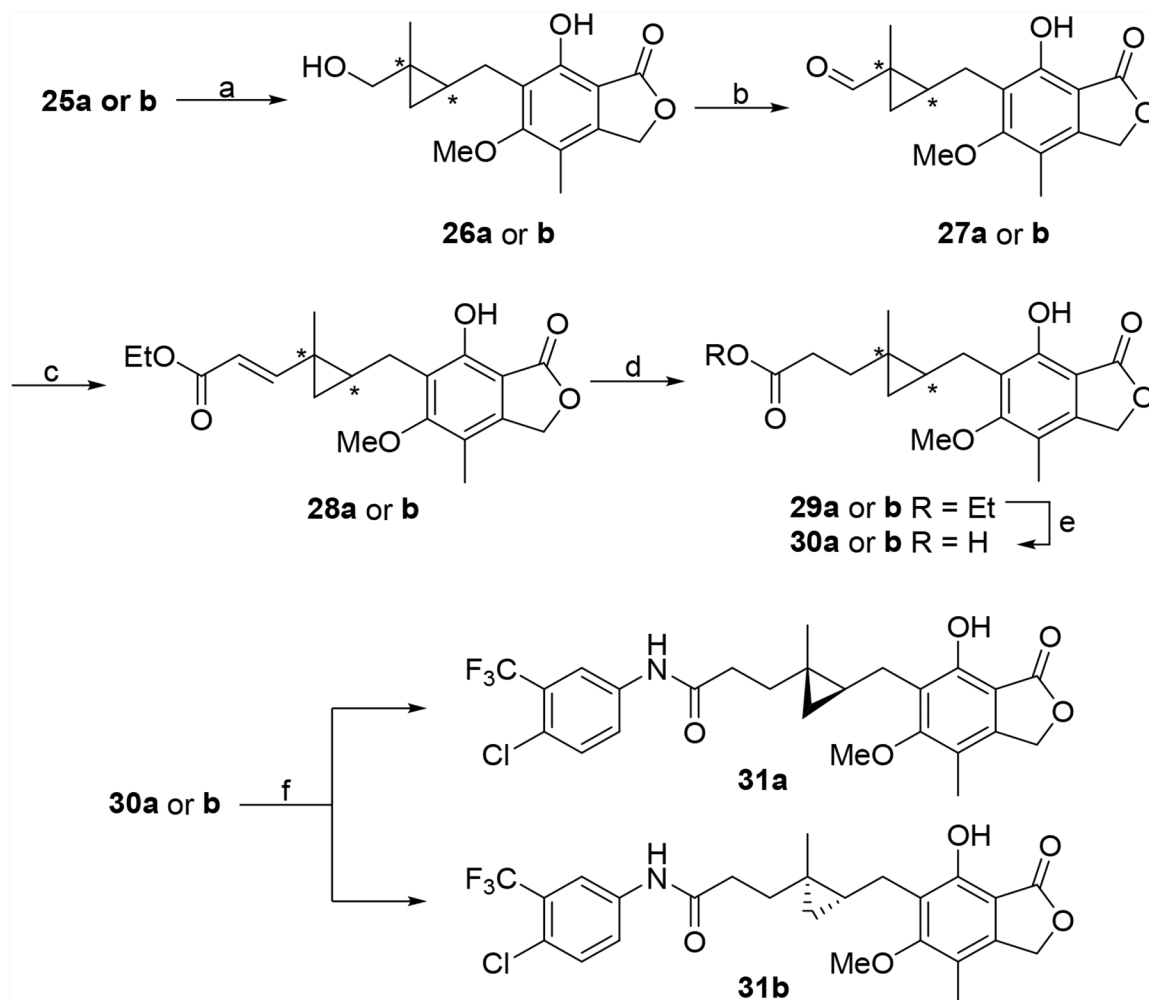
Scheme 1.
Synthesis of **8** – **18**. Reagents and conditions: (a) EDC•HCl, HOBt or HOAt or DMAP, TEA or DIPEA, DMF or DCM, rt or 0 °C to rt, 16 h, 17–80%. (b) i) oxalyl chloride, DMF (cat.), DCM, rt. ii) aniline, TEA, rt, 6 h, 40%. (c) MeI, K_2CO_3, acetone, rt, 16 h, 64%. (d) 10% Pd/C, H_2 (1 atm), EtOAc, rt, 3 h, 34%.
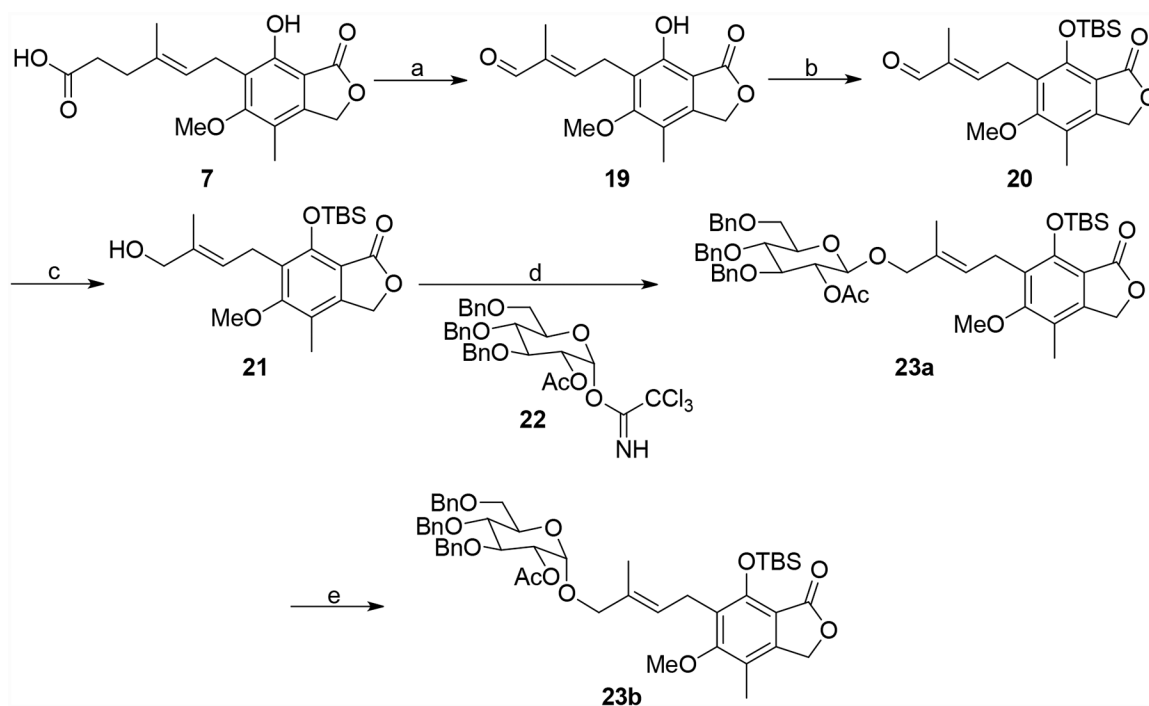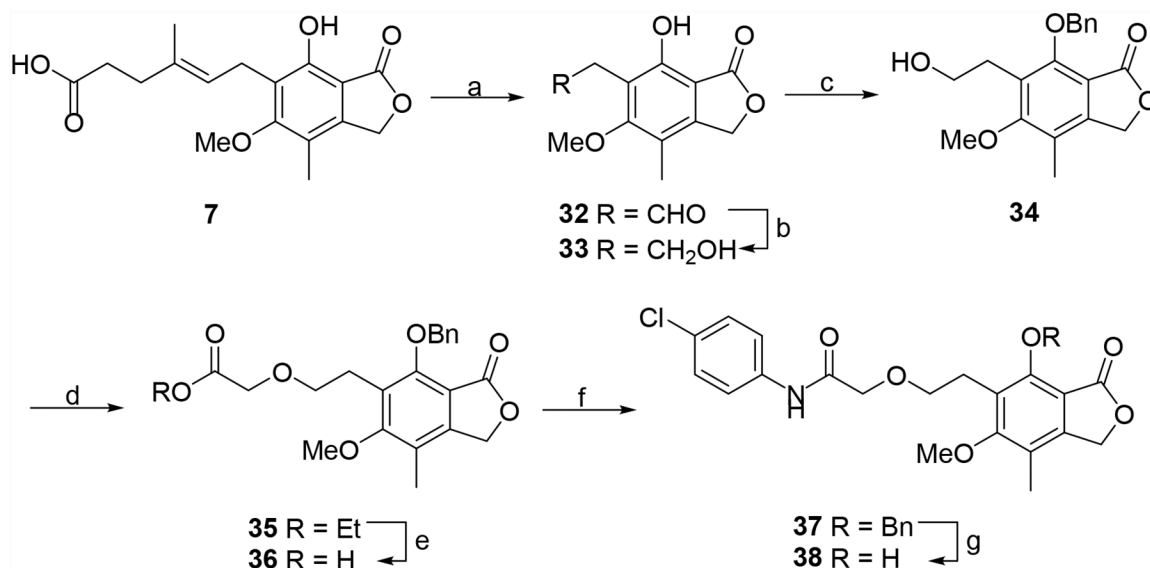
Scheme 2.
Synthesis of intermediates **23a** and **23b**. Reagents and conditions: (a) i) OsO_4, NMO, $NaIO_4$, THF/H_2O, rt, 1.5 h. ii) $PPh_3=C(CH_3)CHO$, benzene, reflux, 24 h, 77%. (b) TBSCl, imidazole, DCM, rt, 16 h, 71%. (c) NaBH, MeOH, 0 °4 C to rt, 1 h, 92%. (d) **22**, $BF_3 \cdot OEt_2$, DCM, −78 °C for 0.5 h then 0 °C for 0.5 h, 88%. (e) $TiCl_4$, DCM, −78°C for 10 min then 0 °C for 0.5 h, 99%.
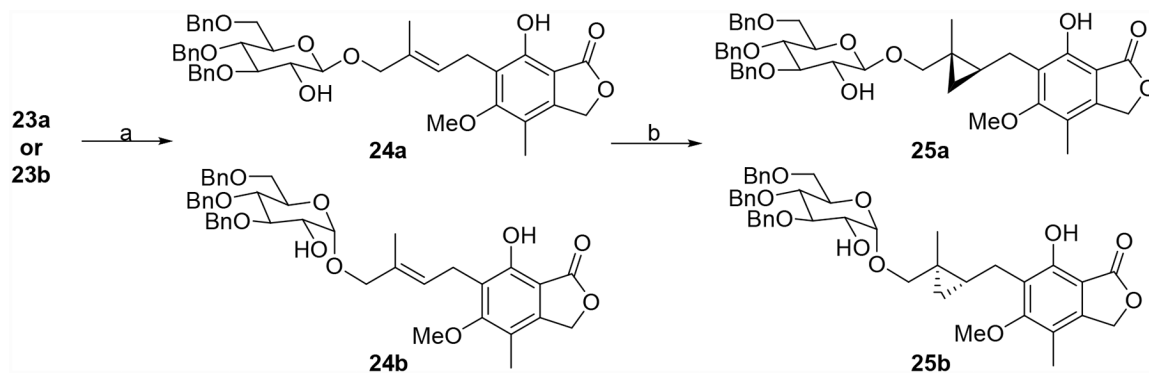
Scheme 3.
Synthesis of intermediates **25a** and **25b**. Reagents and conditions: (a) NaOMe, MeOH, 0 °C to rt, 16 h, 55 and 77%. (b) For **25a**: Et$_2$Zn, CH$_2$I$_2$, toluene, −20 °C, 3 h, 76%. For **25b**: Et$_2$Zn, CH$_2$I$_2$, toluene, −78 °C to rt, 16 h (*dr* 6:1), 98%.

Scheme 4.

Synthesis of **31a** and **31b**. Reagents and conditions: (a) i) Tf$_2$O, pyridine, DCM, −20 °C to rt; ii) DMF, pyridine, H$_2$O, 120 °C, 10 min, 81% and 93%. (b) DMP, DCM, rt, 0.5 h, 99%, and 83%. (c) triethyl phosphonoacetate, NaH, benzene, rt, 1 h, 57% and 51% (d) CoCl$_2$, NaBH$_4$, MeOH/DMF, rt, 0.5 h, 62% and 87% (e) LiOH, THF/H$_2$O, rt, 3 h, 86% and 85%. (f) 4-chloro-3-(trifluoromethyl)aniline, EDC•HCl, HOAt, DMF, rt, 16 h, 81% and 71%.

Scheme 5.
Synthesis of **38**. Reagents and conditions: (a) OsO_4, NMO, $NaIO_4$, THF/H_2O, rt, 1.5 h.
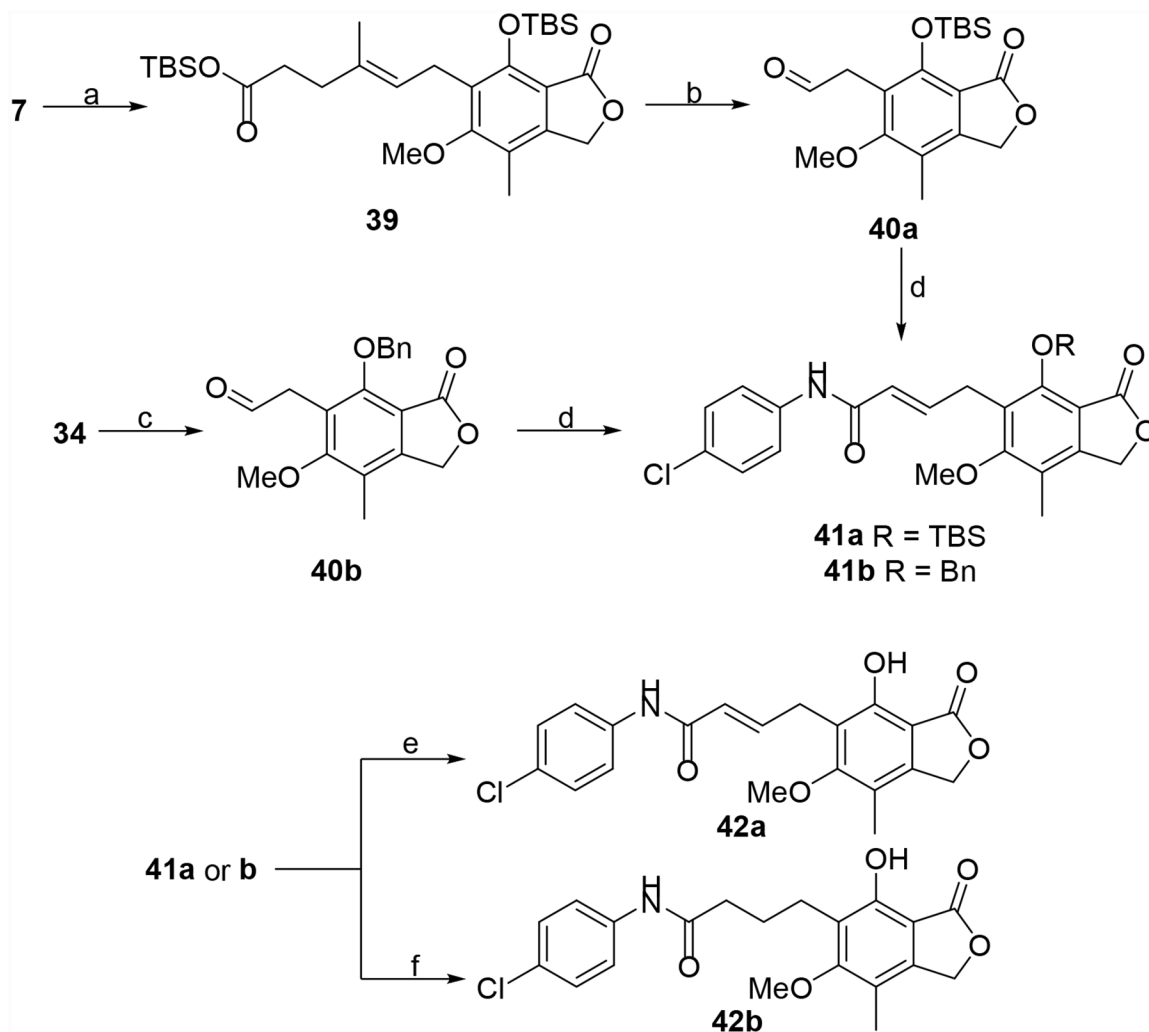(b) $NaBH_4$, EtOH, rt, 3 h, 70–81%. (c) benzyl bromide, TBAF, rt, 6.5 h, 81–89%. (d)
$InCl_3$, ethyl diazoacetate, DCM, rt, 16 h, 57%. (e) LiOH, $MeOH/H_2O$, rt, 3 h, 76–95%.
(f) EDC•HCl, HOAt, 4-chloroaniline, DMF, rt, 16 h, 65–80%. (g) 10% Pd/C, H_2 (1 atm),
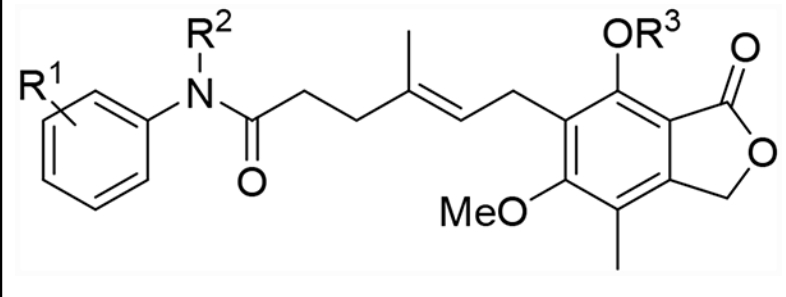MeOH, rt, 1 h, 27–56%.

Scheme 6.
Synthesis of **42a** and **42b**. Reagents and conditions: (a) TBSCl, imidazole, DMF, rt, 6 h, 66%. (b) OsO_4, NMO, $NaIO_4$, THF/H_2O, rt, 1.5 h, 70%. (c) DMP, DCM, rt, 3 h, 80–88%. (d) LDA, 4-ClPhNH(C=O)$CH_2P^+Ph_3Cl^-$ (see Supporting Information compound **S2**), THF/toluene, 0°C to rt, 3 h, 73% and 51% (e) TBAF, THF, 0 °C to rt, 0.5 h, 22% (f) 10% Pd/C, H_2 (1 atm), MeOH, rt, 1 h, 46%.
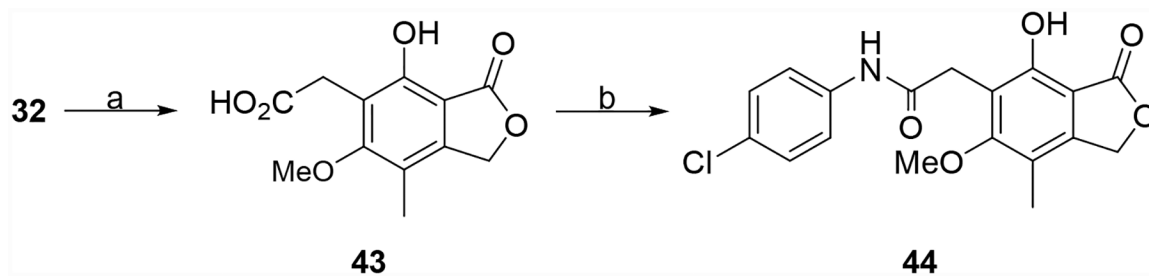
Scheme 7.
Synthesis of **44**. Reagents and conditions: (a) $NaClO_2$, NaH_2PO_4, 2-methyl-2-butene, *t*-BuOH/H_2O, rt, 4 h, 40 mg (b) EDC, DIPEA, 4-chloroaniline, THF/DMF, rt, 16 h, 38%.

Table 1

*Cp*IMPDH and *Hs*IMPDH inhibitory activities of **8** – **17**.

Compound	R¹	R²	R³	*Cp*IMPDH $K_{i,app}$ (μM)	*Hs*IMPDH $K_{i,app}$ (μM)
8	3-OMe, 4-Cl	H	H	0.046 (±0.013)$^\sigma$	0.35 (±0.09)$^\sigma$
9	3,4-di-Cl	H	H	0.041 (±0.010)$^\sigma$	0.34 (± 0.11)$^\sigma$
10	3-CF₃, 4-Cl	H	H	0.016 (±0.007)$^\sigma$	0.23 (±0.08)$^\sigma$
11	2,3-di-Cl	H	H	0.681 (0.143)^r	ND*
12	4-Cl	H	H	0.042 (±0.02)$^\sigma$	0.13 (±0.05)$^\sigma$
13	4-F	H	H	0.180 (±0.06)^r	0.27
14	4-CF₃	H	H	0.151 (±0.04)^r	0.40
15	4-CN	H	H	0.11	0.35
16	4-Cl	Me	H	0.87 (±0.13)^r	ND*
17	3-CF₃ 4-Cl	H	Me	1.7	ND*

*ND: Not Determined

$^\sigma$Standard deviation

^{r}Range

Table 2

CpIMPDH and HsIMPDH inhibitory activities of **18**, **31a**, **31b**, **38**, **42a**, **42b** and **44**.

Compound	R¹	X	CpIMPDH $K_{i,app}$ (μM)	HsIMPDH $K_{i,app}$ (μM)
18	3-CF₃, 4-Cl		0.060 (±0.01)^r	ND*
31a	3-CF₃, 4-Cl		0.57	1.40
31b	3-CF₃, 4-Cl		0.066 (±0.023)^σ	0.46 (±0.28)^σ
38	4-Cl		0.405 (±0.176)^r	0.87
42a	4-Cl		0.48	0.55
42b	4-Cl		0.45 (±0.13)^r	0.29
44	4-Cl		2.8	0.8

* ND: Not Determined

^{σ} Standard deviation

^{r} Range